International Journal of Signal Processing, Image Processing and Pattern Recognition
Vol.9, No.10, (2016), pp.237-248
http://dx.doi.org/10.14257/ijsip.2016.9.10.23

Local Binary Haar Feathers Kadane and Multi-Threshold AdaBoost for Facial Classification and Recognition

Yu Xiang[1]

[1]*Department of Information Technology, Tianjin Chengjian University, Tianjin City, China*
147940866@qq.com

Abstract

A face recognition algorithm based on local binary Haar feathers which represented as Kadane optimizing multi-threshold AdaBoost was proposed according to the problems of texture shape feature representation and classification algorithm accuracy in the process of facial classifying detection and recognition, First, improve the traditional expression by using image Local binary pattern of Haar features , improve image model of texture and shape feature expression ability ; Secondly, for single threshold weak learning algorithm we can not make full use of local binary Haar feature information, resulting in a lower classification accuracy problem proposed Kadane optimizing multi-threshold AdaBoost classifier, to achieve local binary Haar feature representation of facial high accuracy recognition; Finally, through the experiments show, efficient face recognition rate can reach more than 90% by the algorithm,which is superior to the selected comparison algorithm.

Keywords: *Local binary feature; Haar feature; Classifier; Optimization; Face recognition*

1. Introduction

Face detection is a fundamental problem in the field of computer vision. It is widely used in face recognition system, human-computer interaction system and monitoring system [1]. At present, there are many research results, which are devoted to face detection more quickly, more accurate and more convenient to detect system structure and so on. For example, the literature [2] constructs a skin model used to quickly locate candidate face regions. In recent years, research results show that it is an effective way to improve the accuracy of detection by integrating the features of human face into the computation of face detection [3]. In the literature [4], a new method which can quickly adapt to the pretrained classification is proposed, which can not be classified and re trained according to the new test instances, and the results obtained are good. In the document [5], the data mining technology is applied in the face detection task to find the effective edge feature automatically. In practice, the most popular face detection system is usually a trade-off between efficiency and accuracy of face recognition. Because of this, the face detection method based on the Viola-Jones [6] general object detection framework is still widely used today. The computational efficiency of Viola-Jones method is mainly used to reduce the computational complexity of the Haar feature, and the cascade AdaBoost classifier can improve the detection accuracy. The same based on the Viola Jones frame and aiming at the two problems using local binary pattern of Haar features of the traditional expression form is improved, and optimization design of multi threshold AdaBoost classifier based on Kadane and improve the robustness of the model of light interference, and achieve high facial recognition accuracy.

ISSN: 2005-4254 IJSIP
Copyright ⓒ 2016 SERSC

2. Facial Haar Feature Local Binary Pattern

2.1. LBP Feature Extraction

The essence of Local Binary Pattern is a kind of description operator based on local texture feature. Threshold contrast function form of LBP algorithm as below [12]:

$$f\left(I\left(P_i\right),I\left(P_0\right)\right)=\begin{cases}1, if\ I\left(P_i\right)-I\left(P_0\right)\geq T\\0, if\ I\left(P_i\right)-I\left(P_0\right)<T\end{cases} \tag{1}$$

In the equation, $i=1,2,\cdots,8$, Figure 1 (a), as the texture of the original figure, Figure 1 (b) ,as obtain the original texture image through LBP algorithm.

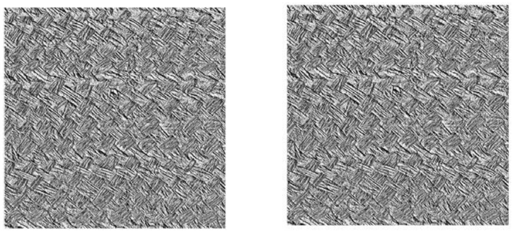

(a) Original image (b) LBP texture image

Figure 1. LBP Algorithm Texture Image

Image $f\left(x,y\right)$'s histogram can be defined as

$$H_i=\sum_{x,y}I\left\{f\left(x,y\right)=i\right\}, i=0,1,\cdots,n-1 \tag{2}$$

$$I\left(x\right)=\begin{cases}1, X=true\\0, X=false\end{cases} \tag{3}$$

Because LBP features are presented in the form of histogram, the difference between different LBP characteristics can be evaluated based on Chi square statistics:

$$\chi^2=\left(S,M\right)=\sum_i\frac{\left(S_i-M_i\right)^2}{S_i+M_i} \tag{4}$$

In the formula, S and M respectively represent two different LBP feature histogram vectors.

2.2. Haar Features

Literature [13] proposed the success of the method lies in: one,use the simple and effective calculation method, namely Haar feature extraction, as shown in Figure 2, the second is the unbalanced structure classification tree, namely the cascade gentle AdaBoost classifier. In the face recognition system, the human face region can be effectively realized based on the image integral, and the Haar feature can be effectively implemented:

$$S'(x',y')=\sum_{x\leq x'}\sum_{y\leq y'}I(x,y) \tag{5}$$

Where (x',y') and(x,y) represents the pixel location. Once an image is obtained by scanning the image once, any Haar feature can be calculated by a very small number of addition and subtraction. Because even in a small image window (for example24*24), it can be detected in the hundreds of thousands of Haar features. Only those which will have

 Copyright ⓒ 2016 SERSC

good discriminative Haar features are selected to construct the unbalanced classification tree.

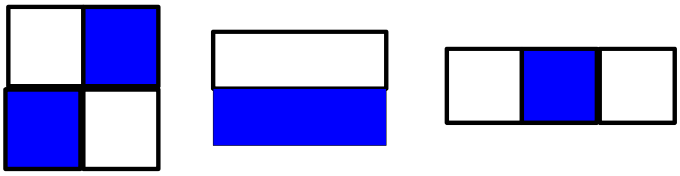

Figure 2. Several Forms of Haar Features

Because the pixel is used as the Haar feature to characterize the image texture, the shape feature of the image can not be obtained, so the LBP operator based on Haar operator is improved.

2.3. HLBP Features

Use the extraction algorithm of construction of HLBP feature based on Haar feature and LBP feature. The specific process is shown in Figure 3, the encoding model diagram is presented in a symmetrical form, and the visible light dark area is converted back to the original shape. There are eight direction the light area center and the center of the model: [180, 225, 270, 315, 0, 45, 90, 135], the regional differences between dark and can represent the texture changes and the information is stored in the center model HLBP feature values.

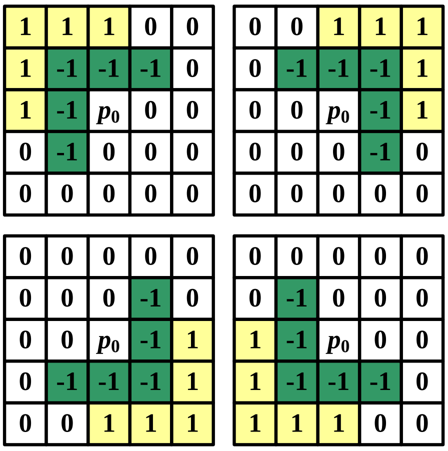

Figure 3. HLBP Feature Encoding Model

Figure 3, HLBP feature coding model, the dark squares setting value is - 1, the light colored squares setting value is 1, the white squares setting value is 0, the coding model center is recording the change of texture of the Haar feature of face. In the image of any pixel in the window of the HLBP value calculation:

$$S(x,y)=HLBP\left(I(x,y)\right)=\sum_{k=1}^{8}B\left(M_k\cdot W(x,y)\right)\times 2^{8-k} \tag{6}$$

In the formula, the calculation form of the window parameters $W(x,y)$ and M_k are referred to the literature [13].

3. Single Threshold Weak Classifier Cascade Face Detection

3.1. Gentle AdaBoost Learning

Each node classifier in the classification tree is known as the first level classification, and is constructed by Gentle AdaBoost learning. In the literature [6], the weak classifier is designed to be a simple function of a single threshold based on a single Haar feature in the classification stage. In general, for a given training sample:

$$X \times Y = \{(\mathbf{x}_k, y_k) \mid k = 1, 2, \cdots, N\} \tag{7}$$

In the formula, $\mathbf{x}_k \in R^m$, $y_k \in Y = \{-1, +1\}$, if the k example $(\mathbf{x}_k, y_k)$ is positive , $y_k = +1$, otherwise $y_k = -1$. In this paper, we use $[\mathbf{x}_k]_j$ represents the J Haar feather in k instance example $(\mathbf{x}_k, y_k)$, and the order indicates that $H_j = \{[\mathbf{x}_k]_j\}$ represent the j Haar feature value assembly. According to the Haar value assembly, the training samples can be divided into 2 parts by a single threshold. The optimal threshold value can be determined by minimizing the weighted error. Then, the weak classifier can be defined as:

$$h_j(x) = \begin{cases} 1, & p_j[\mathbf{x}]_j < p_j\theta_j \\ 0, & \text{otherwise} \end{cases} \tag{8}$$

In the formula, $\mathbf{x}$ represents observed value of the test case , $[\mathbf{x}]_j$ represents the j Haar characteristic value, p_j indicates the polarity of the weak classifies $p_j \in \{1, -1\}$. In the process of calculation of the optimal threshold θ_j, the corresponding eigenvalue is $[\mathbf{x}_k]_j$ first calculated and descending order, for example: $\left([\mathbf{x}_1]'_j, \cdots, [\mathbf{x}_m]'_j, \cdots, [\mathbf{x}_n]'_j, \cdots, [\mathbf{x}_N]'_j\right)$, in which , $[\mathbf{x}_m]'_j \le [\mathbf{x}_n]'_j$, $1 \le m < n \le N$. For a numeric consisting of a sorted list, the maximum $N+1$ potential of the threshold position is expressed , because this characteristic value is usually different, for example, the first threshold selection corresponds to, as well as the special case: $\bar{\theta}_{j0} < [\mathbf{x}_1]'_j$, $\bar{\theta}_{jN} > [\mathbf{x}_N]'_j$.

3.2. Optimal Threshold Determination

Assume T^+ as the sum of the weights of all positive instances, T^- as the sum of the weights of all the negative examples, is $T^+ + T^- = 1$. For a given threshold $\bar{\theta}_{ji}$,order S_{ji}^+ as the sum of the weights of all positive instances below the threshold value, indicating that the sum of the weights of all the negative examples below the threshold value $\bar{\theta}_{ji}$. Assuming S_{ji}^- as a weak classification function is defined $[\mathbf{x}]_j < \bar{\theta}_{ji}$, then $\mathbf{x}$ positive, otherwise $\mathbf{x}$ negative. The sum of the classification errors is the sum of positive and negative examples $T^- - S_{ji}^-$. For the definition of weak classification function, we can use the same method to calculate the corresponding classification error $S_{ji}^- + (\mathrm{T}^+ - \mathrm{S}_{ji}^+)$. Based on the previous analysis, the minimum weighted error can be evaluated:

$$e_j = \min_i \left(S_{ji}^+ + (T^- - S_{ji}^-), S_{ji}^- + (T^+ - S_{ji}^+)\right) \tag{9}$$

The corresponding optimal threshold:

$$\hat{i} = \arg\min_i \left(S_{ji}^+ + (T^- - S_{ji}^-), S_{ji}^- + (T^+ - S_{ji}^+)\right) \tag{10}$$

 Copyright ⓒ 2016 SERSC

Under the optimal threshold, if the condition meet: $S_{ji}^{+}+(T^{-}-S_{ji}^{-})\geq S_{ji}^{-}+(T^{+}-S_{ji}^{+})$, then $p_j=1$; or $p_j=-1$.In addition, the best features can be determined according to its index:

$$\hat{j}=\arg\min\ e_j \tag{11}$$

4. Multi-Threshold Weak Classifier

4.1. Kadane Calculation of Threshold

Because the single threshold weak learning can not make full use of the Haar feature information, it can not adapt to the sample distribution in the feature space, which result in low classification accuracy. For this shortcoming, a multi threshold weak classifier is used, and an intelligent selection method based on the optimal threshold is designed. In addition, a classification optimization problem is proposed based on the Kadane algorithm, and the computational complexity of the multi threshold algorithm is a linear increase of the computational complexity of the single threshold weak classifier. Based on the threshold value obtained by the Kadane algorithm, the feature space can be divided into 5 sub spaces at most, and the corresponding weak classification function can be defined by the evaluation of each classification range.

In the proposed algorithm, the given Haar feature is divided into 3 parts. The corresponding interval range can be divided into three regions, the leading region of the positive example, the dominant area of the negative example and the uncertain region. The regions are called: PR region, NR region and UR region. The specific location of the relationship as shown in Figure 4.

The θ_l^{+} and θ_r^{+} corresponding positive instance dominant regions respective left and right boundaries, respectively, The θ_l^{+} and θ_r^{+} corresponding negative instance dominant regions respective left and right boundaries.For the single threshold weak classifier, because there is only a potential $N+1$ threshold position, we can use the linear complexity $O(N)$ to complete the optimal threshold calculation, which N is the number of examples in the training samples. However, to determine the positive range and the negative range boundary, if a similar approach is used, there is potential $N(N+1)/2$ positive and negative range case to be considered $O(N^2)$. For Haar features, it is effective to calculate the positive range and the negative range boundary, which is usually converted into the following optimization problems:

$$\begin{cases} P1=\max\limits_{\theta_l^{+},\theta_r^{+}} \sum\limits_{\theta_l^{+}\leq[\mathbf{x}_k]_j\leq\theta_r^{+}} w_k y_k \\ P2=\min\limits_{\theta_l^{-},\theta_r^{-}} \sum\limits_{\theta_l^{-}\leq[\mathbf{x}_k]_j\leq\theta_r^{-}} w_k y_k \end{cases} \tag{12}$$

In the formula, the weight of the instance k is expressed as w_k, the optimization problem can be calculated by the Kadane algorithm, and the goal is to find the maximum sub array which contains the positive and negative one dimensional array to be realized. The time complexity of the Kadane algorithm is $O(N)$, in which N is the length of the one dimension array. Obviously, the problem P1 is equivalent to solving the problem of the sum of the maximal sub arrays, which is similar to that of P2, which can be transformed into the maximum optimization problem.

Copyright ⓒ 2016 SERSC

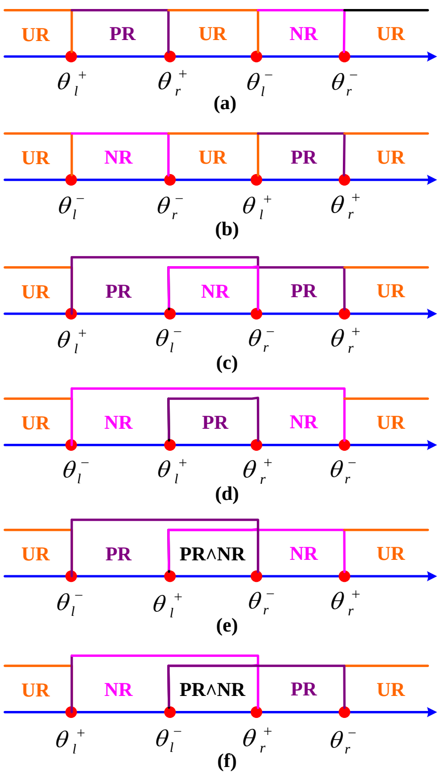

Figure 4. Positive and Negative Instances of the Dominant Regional Position

Simple application of Kadane algorithm to find the positive range and negative range boundary, that is, the weak classifier threshold. Specific, for the Haar feature H, first of all the feature list were in ascending order, similar single threshold weak classifiers to construct the way and the appropriate weights and training examples, (w'_k, y'_k) , $k = 1, 2, \cdots, N$. Then, the Kadane algorithm is used to obtain the optimal solution (l^+, r^+) and (l^-, r^-) of the problem P1 and the problem P2, in which l^+ and r^+ the left and right of the negative range are expressed. Finally, the threshold value is evaluated by selecting the characteristic value of the boundary and the adjacent region of the characteristic value:

$$\theta_l^+ = \frac{[\mathbf{x}_{l^+}]'_j + [\mathbf{x}_{l^+-1}]'_j}{2} \tag{13}$$

$$\theta_r^+ = \frac{[\mathbf{x}_{r^+}]'_j + [\mathbf{x}_{r^++1}]'_j}{2} \tag{14}$$

$$\theta_l^- = \frac{[\mathbf{x}_{l^-}]'_j + [\mathbf{x}_{l^--1}]'_j}{2} \tag{15}$$

$$\theta_r^- = \frac{[\mathbf{x}_{r^-}]'_j + [\mathbf{x}_{r^-+1}]'_j}{2} \tag{16}$$

Copyright ⓒ 2016 SERSC

Algorithm 1: calculate the positive and negative range of the first Haar eigenvalue H_j.

Input: training data $\{([\mathbf{x}_k]_j, y_k, w_k) | k = 1,2,\cdots,N\}$;

Output: positive range $[\theta_l^+, \theta_r^+]$ and negative range $[\theta_l^-, \theta_r^-]$;

$([\mathbf{x}_k]'_j, y'_k, w'_k) | k = 1,2,\cdots,N$, $[\mathbf{x}_m]'_j \le [\mathbf{x}_n]'_j$, $1 \le m \le n \le N$ 。

Step 1: according to the increasing order $[\mathbf{x}_k]_j$ classifying the training data , and obtain: ：

$([\mathbf{x}_k]'_j, y'_k, w'_k) | k = 1,2,\cdots,N$, in which $[\mathbf{x}_m]'_j \le [\mathbf{x}_n]'_j$, $1 \le m \le n \le N$.

, $(l^-, r^-, c^-, l_n^-, s^-) := (0,0,0,1,0)$

for $i = 1,2,\cdots,N$ do

$c^+ := c^+ + w'_i y'_i$, $c^- := c^- + w'_i y'_i$ ；

if $c^+ > s^+$ then

$s^+ := c^+$; $(l^+, r^+) := (l_p^+, i)$;

end

if $c^+ < 0$ then

$c^+ := 0$; $l_p^+ := i + 1$;

end

if $c^- < s^-$ then

$s^- := c^-$; $(l^-, r^-) := (l_n^-, i)$;

end

if $c^- > 0$ then

$c^- := 0$; $l_n^- := i + 1$;

end

end

Step 3：Output threshold：

$[\theta_l^+, \theta_r^+] = [\frac{[\mathbf{x}_{l^+}]'_j + [\mathbf{x}_{l^+-1}]'_j}{2}, \frac{[\mathbf{x}_{r^+}]'_j + [\mathbf{x}_{r^++1}]'_j}{2}]$

$[\theta_l^-, \theta_r^-] = [\frac{[\mathbf{x}_{l^-}]'_j + [\mathbf{x}_{l^--1}]'_j}{2}, \frac{[\mathbf{x}_{r^-}]'_j + [\mathbf{x}_{r^-+1}]'_j}{2}]$

4.2. Multi-Threshold Weak Classifier

In the literature [6], it points out that the performance of AdaBoost Gentle algorithm is better than the discrete AdaBoost algorithm and real number AdaBoost algorithm, so the AdaBoost Gentle algorithm is used to construct a strong classifier. According to the above, a plurality of thresholds can be determined based on the following parameters θ_l^- 、 θ_r^- 、 θ_l^+ and θ_r^+ as well as restrictions and conditions $\theta_l^- \le \theta_r^-$ and $\theta_l^+ \le \theta_r^+$. The 4 threshold parameters can be divided into 5 sub ranges of one dimensional space. Clearly in the restrictions and conditions, the existence, and the 6 kinds of interval division of the location of θ_l^- 、 θ_r^- 、 θ_l^+ and θ_r^+, as shown in Figure 1. Therefore, there are six possible relationships between the positive range $[\theta_l^+, \theta_r^+]$ and the negative range $[\theta_l^-, \theta_r^-]$. But it can be theoretically proved that (e) and (f) two kinds of situations are not possible.

Proof: because, $[\theta_l^+, \theta_r^+]$ and $[\theta_l^-, \theta_r^-]$ respectively are the optimal solution to the problem P1 and problem P2 , order , 令 $\alpha = \sum_{\theta_l^+ \le [\mathbf{x}_k]_j \le \theta_r^+} \omega_k y_k$, $\beta = \sum_{\theta_l^- \le [\mathbf{x}_k]_j \le \theta_r^-} \omega_k y_k$, then there is:

$$\begin{cases} \alpha = \sum\limits_{\theta_l^+ < [\mathbf{x}_k]_j \le \theta_l^-} w_k y_k + \sum\limits_{\theta_l^- < [\mathbf{x}_k]_j < \theta_r^+} w_k y_k \\ \beta = \sum\limits_{\theta_l^- < [\mathbf{x}_k]_j < \theta_r^+} w_k y_k + \sum\limits_{\theta_r^+ \le [\mathbf{x}_k]_j < \theta_r^-} w_k y_k \end{cases} \tag{17}$$

Because $\alpha > \sum_{\theta_l^+ < [\mathbf{x}_k]_j \le \theta_l^-} w_k y_k$, according to the formula(12)we can get $\sum_{\theta_l^- < [\mathbf{x}_k]_j < \theta_r^+} w_k y_k > 0$ .Similarly, according to $\beta < \sum_{\theta_r^+ \le [\mathbf{x}_k]_j < \theta_r^-} w_k y_k$, there is

$\sum_{\theta_l^- < [\mathbf{x}_k]_j < \theta_r^+} w_k y_k < 0$.Based on the assumption that there is a contradiction, the situation(f) is not possible. In the absence of the same syndrome (e).

Gentle AdaBoost requires each weak classifier to have confidence in the output. As shown in Figure 1, through the observation of training samples, the positive range of the positive range of samples is higher than the negative range of the probability of positive output samples, negative range of confidence in the negative range of the output probability is higher than the positive range of samples. Therefore, for a multi threshold definition interval $[u,v]$, the confidence function of the characteristic is corresponding to the characteristic $C_j(u,v)$ is.

$$C_j(u,v) = \frac{\sum_{u \le [\mathbf{x}_k]_j \le v} w_i y_i}{\sum_{u \le [\mathbf{x}_k]_j \le v} w_i} \tag{18}$$

The weak classifier function of the first Haar feature is represented by the piecewise function $g_j(\mathbf{x})$. In Figure two cases (a) (b) , can be defined as a function of the form:

$$g_j(x) = \begin{cases} C_j\left(\theta_l^+, \theta_r^+\right), \theta_l^+ \le [\mathbf{x}]_j \le \theta_r^+ \\ C_j\left(\theta_l^-, \theta_r^-\right), \theta_l^- \le [\mathbf{x}]_j \le \theta_r^- \\ C_j(-\infty, \min(\theta_l^-, \theta_l^+)), [\mathbf{x}]_j < \min(\theta_l^-, \theta_l^+) \\ C_j(\max(\theta_r^+, \theta_r^-), +\infty), [\mathbf{x}]_j > \max(\theta_r^+, \theta_r^-) \\ 0, otherwise \end{cases} \tag{19}$$

According to the formula (13), the confidence values of different ranges can be got. It should be noted that the positive and negative range is defined as zero. In fact, it can be proved in the form of mathematical deduction. For the case (a), it is assumed that there are two possible:

$$\begin{cases} \sum_{\theta_r^+ < [\mathbf{x}_k]_j < \theta_l^-} w_k y_k > 0 \\ \sum_{\theta_r^+ < [\mathbf{x}_k]_j < \theta_l^-} w_k y_k < 0 \end{cases} \tag{20}$$

If meet $\sum_{\theta_r^+ < [\mathbf{x}_k]_j < \theta_l^-} w_k y_k > 0$,we get：

$$\sum_{\theta_l^+ \le [\mathrm{x_k}]_j < \theta_l^-} \mathrm{w_k y_k} = \alpha + \sum_{\theta_r^+ < [\mathbf{x}_k]_j < \theta_l^-} w_k y_k > \alpha \tag{21}$$

This means θ_l^+ and θ_r^+ P1 are not the optimal solution .In the same way we know that if meet $\sum_{\theta_r^+ < [\mathbf{x}_k]_j < \theta_l^-} w_k y_k < 0$ then θ_l^-, θ_r^- are not the optimal solution to P2.then the above assumption is not true， we know $\sum_{\theta_r^+ < [\mathbf{x}_k]_j < \theta_l^-} w_k y_k = 0$ .According to formula(13), the confidence interval of the interval is zero.This case also applied for Figure 1(b).

According to the fig1 case(c),weak classifier function can be defined as the form:

$$g_j(\mathbf{x}) = \begin{cases} C_j(-\infty, \theta_l^+), [\mathbf{x}]_j < \theta_l^+ \\ C_j\left(\theta_l^+, \theta_l^-\right), \theta_l^+ \le [\mathbf{x}]_j < \theta_l^- \\ C_j(\theta_l^-, \theta_r^-), \theta_l^- \le [\mathbf{x}]_j \le \theta_r^- \\ C_j\left(\theta_r^-, \theta_r^+\right), \theta_r^- < [\mathbf{x}]_j \le \theta_r^+ \\ C_j(\theta_r^+, +\infty), [\mathbf{x}]_j > \theta_r^+ \end{cases} \tag{22}$$

According to the Figure 1 case(d),weak classifier function can be defined as the form:

 Copyright ⓒ 2016 SERSC

$$g_j(x)=\begin{cases} C_j(-\infty,\theta_l),[\mathbf{x}]_j<\theta_l^- \\ C_j\left(\theta_l^-,\theta_l^+\right),\theta_l^-\le[\mathbf{x}]_j<\theta_l^+ \\ C_j\left(\theta_l^+,\theta_r^+\right),\theta_l^+\le[\mathbf{x}]_j\le_r^+ \\ C_j\left(\theta_r^+,\theta_r^-\right),\theta_r^+<[\mathbf{x}]_j\le\theta_r^- \\ C_j(\theta_r^-,+\infty),[\mathbf{x}]_j>\theta_r^- \end{cases} \tag{23}$$

Using squared error function:

$$\varepsilon_j=\sum_{k=1}^{N}w_k(g_j(\mathbf{x}_k)-y_k)^2 \tag{24}$$

Based on (19) squared error function, the classification performance of weak classifier is evaluated, which ε_j indicates the training error of the weak classifier. For each stage of the AdaBoost Gentle algorithm, the minimum weight error of the weak classifier is chosen as the parameters of the cascade classifier.

5. Experimental Analysis

Experiment 1: (classifier performance test) here to prepare 10000 positive examples and 10000 negative examples as the training data, and each instance of the size of 24 x 24 pixels. The Adaboost gentle algorithm is used to generate two strong classifiers, each of which consists of 100 weak classifiers. A classifier is trained using the weak classifier learning algorithm, and the other classifier is trained using the single threshold weak classifier learning algorithm.

Order the strong classifier, $G(\mathbf{x})=sign\left(\sum_{t=1}^{M}h_t(\mathbf{x})-b\right)$, the detection rate of the 2 classifiers can be obtained by adjusting the threshold parameters, such as the false alarm rate curve (FAR) and the detection rate curve (DA). 10000 positive examples and 10000 negative examples are selected as the test data. The simulation results are shown in Figure 5.

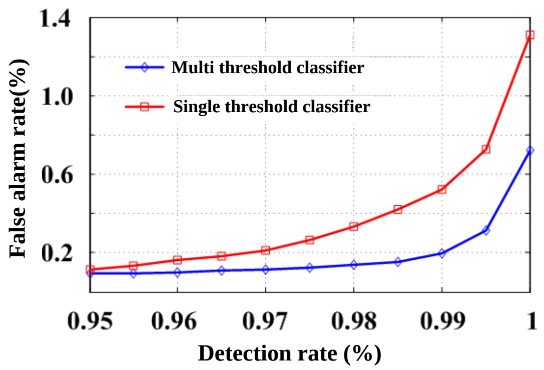

Figure 5. Performance Curve of Detection Rate False Alarm Rate

Figure 5, contrast curve showed that, under the same detection rate and the Titus threshold classifier false alarm rate is lower than the single threshold classifier of the false alarm rate. This shows that the multi threshold weak classifier has stronger recognition ability than the single threshold weak classifier.

Experiment 2 (feature extraction performance test) here is to select the Brodatz texture scale transform library classification experiments, verify the effectiveness of the method of feature extraction. The Brodatz contains 32 pieces of texture are texture pixels. Each texture is divided into 16 different size is the size of the image, the first use of histogram equalization to remove the sample brightness difference. In addition, 3 sets of auxiliary samples were generated for each sample rotation. To enlarge the image of the original sample image center into a pixel image, the process can be obtained through the process of rotating and enlarged image test training samples (shown in Figure 6). A total of 2048 sets of test training samples were obtained from the above mentioned samples. Select 32 groups of samples from each of the above categories as the training set, the other selected 32 sets of samples as a test set.

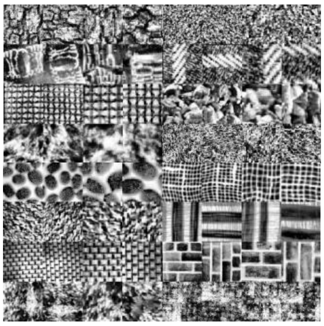

Figure 6. Brodatz Texture Library Sample

Experimental results as shown in Table 1, below, HLBP feature extraction than using LBP feature extraction and recognition accuracy is improved based on, in terms of computational efficiency in 2048 samples Gallery the time-consuming long increase about 1s, per sample images increases when the length is about 0.5ms, based on LDP feature extraction and the recognition rate is 85.73%, but the computation time increased to about 155.84s calculated price is not high. Next, after using the Gabor+LBP algorithm, the recognition rate is increased to 91.12%, but the computation time is greatly increased to 573.16s. And the Gabor+HLBP algorithm relative to Gabor+LBP algorithm recognition rate has improved, and the computation time is reduced to 284.31s. Gabor+HLBP algorithm and Gabor+LBP algorithm in the increase of normalized operation, the calculation of long time changes, but the algorithm recognition rate has declined, it is not necessary for the feature extraction and recognition.

Table 1. Performance Comparison of Feature Extraction

Algorithm	Correct rate(%)	Time(s)
LBP	82.92	36.64
LDP	85.73	155.84
HLBP	87.89	37.69
Gabor+LBP	91.12	573.16
Norm+Gabor+LBP	90.73	579.27
Gabor+HLBP	92.86	284.31
Norm+Gabor+HLBP	91.69	281.65

6. Conclusion

In this paper, based on the local binary Haar feature representation, the Kadane optimal multi threshold AdaBoost face recognition algorithm is proposed, which can improve the efficiency of the feature extraction and improve the accuracy of classification. The experimental results show that the proposed algorithm can improve the performance of the proposed algorithm , and the performance of the algorithm is improved compared with the literature. In this paper, by using contrast in the experimental stage clean background standard database as the experimental object, in the design phase of the algorithm also does not take into account the image background, research on how to effectively enhance

Copyright ⓒ 2016 SERSC

the complex environment under the background of face recognition accuracy remains to be the subject of further research.

Acknowledgement

The research is supported by Tianjin Xinghai plan(KJXH2014-13).

References

[1] J. Hu and Z. Gao, "Modules identification in gene positive networks of hepatocellular carcinoma using Pearson agglomerative method and Pearson cohesion coupling modularity", Journal of Applied Mathematics, vol. 2012, **(2012)**.

[2] Y. Geng, J. Chen, R. Fu, G. Bao and K. Pahlavan, "Enlighten Wearable Physiological Monitoring systems:",On-Body RF Characteristics Based Human Motion Classification Using a Support Vector Machine. PP99), **(2015)**, pp. 1-16.

[3] X. Song and Y. Geng, "Distributed Community Detection Optimization Algorithm for Complex Networks", Journal of Networks, vol. 9, no. 10, **(2014)**, pp. 2758-2765.

[4] K. Pahlavan, P. Krishnamurthy and Y. Geng, "Localization Challenges for the Emergence of the Smart World", Access, IEEE, vol. 3, no. 1, **(2015)**, pp. 1-11.

[5] J. He, Y. Geng, Y. Wan, S. Li, and K. Pahlavan, "A cyber physical test-bed for virtualization of RF access environment for body sensor network", Sensors Journal, IEEE, vol. 13, no. 10, **(2013)**, pp. 3826-3836.

[6] Z. Lv, A. Tek and F. D. Silva, "Game on, science-how video game technology may help biologists tackle visualization challenges", PloS one, vol. 8, no. 3, **(2013)**, pp. 57990.

[7] T. Su, W. Wang and Z. Lv, "Rapid Delaunay triangulation for randomly distributed point cloud data using adaptive Hilbert curve", Computers & Graphics, vol. 54, **(2016)**, pp. 65-74.

[8] J. Hu, Z. Gao and W. Pan, "Multiangle Social Network Recommendation Algorithms and Similarity Network Evaluation", Journal of Applied Mathematics, vol. 2013, **(2013)**.

[9] S. Zhou, L. Mi, H. Chen and Y. Geng, "Building detection in Digital surface model", 2013 IEEE International Conference on Imaging Systems and Techniques (IST), **(2012)** October.

[10] J. He, Y. Geng and K. Pahlavan, "Toward Accurate Human Tracking: Modeling Time-of-Arrival for Wireless Wearable Sensors in Multipath Environment", IEEE Sensor Journal, vol. 14, no. 11, **(2014)** November, pp. 3996-4006.

[11] Z. Lv, A. Halawani and S. Fen, "Touch-less Interactive Augmented Reality Game on Vision Based Wearable Device", Personal and Ubiquitous Computing, vol. 19, no. 3, **(2015)**, pp. 551-567.

[12] G. Bao, L Mi, Y. Geng, M. Zhou and K. Pahlavan, "A video-based speed estimation technique for localizing the wireless capsule endoscope inside gastrointestinal tract", 2014 36th Annual International Conference of the IEEE Engineering in Medicine and Biology Society (EMBC), **(2014)** August.

[13] D Zeng and Y. Geng, "Content distribution mechanism in mobile P2P network", Journal of Networks, vol. 9, no. 5, **(2014)** January, pp. 1229-1236.

Author

Yu Xiang, received her M.S. degree in internet engineering from Estonian Business School of Information Technology and Telecommunications in Tallinn, Estonia. He is currently a lecturer in Tianjin Cheng Jian University. His research interest is mainly in the area of Computer Software, Internet and Electrical Integration. He has published several research papers in scholarly journals in the above research areas and has participated in several books.

Copyright ⓒ 2016 SERSC